Applied Materials Today 50 (2026) 103191

Contents lists available at ScienceDirect

Applied Materials Today

journal homepage: www.elsevier.com/locate/apmt

Chitosan-based nanoemulsions as eugenol/hexyl gallate delivery systems against *Xanthomonas citri*

Jaiber Humberto Rodriguez Llanos [a,*], Eddyn Gabriel Solorzano Chavez [a], Danieli Fernanda Canaver Marin [a], Rayane Monique Sete da Cruz [a,b], Vitor Rodrigues Marin [b], Caio Felipe Cavicchia Zamuner [b], Terezija Jovanovski [d,e], Geovanny Barroso [b], Osmar Malaspina [b], Peter J. Deuss [e], Dirk-Jan Scheffers [d], Samantha Cristina de Pinho [c], Andrij Pich [f,g,h], Henrique Ferreira [b,*], Michel Brienzo [a,*]

[a] São Paulo State University (UNESP), Institute for Research in Bioenergy (IPBEN), R. 10, 2527, Rio Claro, SP 13500–230, Brazil
[b] São Paulo State University (UNESP), Institute of Bioscience (IB), Department of General and Applied Biology, Av. 24 A, Rio Claro, SP 13506–900, Brazil
[c] Department of Food Engineering, School of Animal Science and Food Engineering (FZEA), University of SÃo Paulo, R. Duque de Caxias, 225, Pirassununga, SP 13635–900, Brazil
[d] Department of Molecular Microbiology, Groningen Biomolecular Sciences and Biotechnology Institute, University of Groningen, Groningen 9747 AG, the Netherlands
[e] Green Chemical Reaction Engineering (ENTEG), University of Groningen, Nijenborgh 3, Groningen 9747 AG, the Netherlands
[f] DWI–Leibniz Institute for Interactive Materials, RWTH Aachen University, Forckenbeckstraße 50, Aachen 52074, Germany
[g] Institute of Technical and Macromolecular Chemistry, RWTH Aachen University, Worringerweg 2, 52074 Aachen, Germany
[h] Aachen-Maastricht Institute for Biobased Materials, University of Maastricht, Brightlands Chemelot Campus, Urmonderbaan 22, 6167 RD Geleen, the Netherlands

ARTICLE INFO

Keywords:
Nanoemulsions
Chitosan
Microbial control
Sustainable agriculture
Xanthomonas citri

ABSTRACT

Two systems of nanoemulsions encapsulating hexyl gallate-eugenol (GaOi) were developed for sustainable plant protection. A water-based system (GaOi-Water, F24) and a 1 % (w/v) chitosan-stabilized system (GaOi-Qs, F64) were prepared using high-energy emulsification and analyzed using DLS, AFM, and TEM. F24 displayed narrowly distributed spherical droplets (AFM: 40–150 nm; DLS mean ~140 nm; PDI <0.3), whereas F64 formed a chitosan-encapsulated core–shell network with larger aggregates (>400 nm) embedding smaller nanodomains (20–50 nm), consistent with a polymeric shell that may confer sustained-release kinetics. Transmission electron microscopy corroborated these architectures, showing well-defined core-shell morphologies that correlated with the sustained release behavior of F64. In addition, F64 exhibited high encapsulation efficiency and pronounced colloidal stability ($|\zeta| > 50$ mV). Functionally, microbroth (REMA) assays showed that F64 was an order of magnitude more potent than F24 (IC_{90}/MBC: 0.03125 %, 0.125 % v/v), an effect attributed to the potential disruption of the membrane by possible synergistic interaction and the prolonged availability of the antifungal on the surface. Crucially, acute ecotoxicity tests on two stingless bee species (*Melipona scutellaris* and *Scaptotrigona postica*) revealed no mortality or feeding impairment at active doses. Greenhouse trials on sweet orange demonstrated lesion reductions comparable to commercial copper sprays, using markedly lower active loads. Thus, the results link nano-architecture to release behavior and biological outcomes, illustrating a materials-driven pathway for high-efficacy, pollinator-safe crop protection. The GaOi-chitosan system represents a scalable and environmentally sound alternative to metal-based bactericides with strong potential for field translation.

1. Introduction

Nanoemulsions are colloidal systems that encapsulate and can release bioactive compounds in a controlled and efficient manner. They are versatile technologies on a nanometric scale, providing properties such as high physical stability, capacity to incorporate hydrophobic substances, and able to enhance the bioavailability of the active compounds [30]. In addition, the simplicity of synthesis and versatility have

* Corresponding authors.
E-mail addresses: jaiber@unicamp.br (J.H.R. Llanos), henrique.ferreira@unesp.br (H. Ferreira), michel.brienzo@unesp.br (M. Brienzo).

https://doi.org/10.1016/j.apmt.2026.103191
Received 1 December 2025; Received in revised form 26 February 2026; Accepted 12 March 2026
Available online 18 March 2026
2352-9407/© 2026 The Authors. Published by Elsevier Ltd. This is an open access article under the CC BY license (http://creativecommons.org/licenses/by/4.0/).

expanded their use in industrial and agricultural applications, making nanoemulsions an attractive and sustainable approach [2]. Nanoemulsions could offer significant potential for controlling microorganisms, especially phytopathogens such as *Xanthomonas* spp. This group of bacteria is responsible for serious economic losses in crops of high agricultural importance such as citrus fruits (*X. citri*) and vegetables [4].

Hexyl gallate, an ester derivative of gallic acid, has demonstrated broad-spectrum antimicrobial activity against gram-negative bacteria by permeabilizing the outer membrane and inducing oxidative stress within the cell [31,37]. Its lipophilicity allows it to integrate more readily into lipid bilayers, increasing its ability to reach and destabilize the bacterial membrane. Nanoemulsions that combine natural antimicrobial compounds, such as hexyl gallate, eugenol, and chitosan, offer a dual mechanism of action. Hexyl gallate, when combined with eugenol in formulations, not only amplifies the immediate bactericidal effect due to additive membrane disruption but also acts together to decrease the growth and development of pathogens through its free radical scavenging properties, which attenuate microbial defense mechanisms [4]. By encapsulating hexyl gallate and eugenol in a chitosan matrix, sustained-release kinetics are possible, as inhibitory concentrations can be maintained on the leaf surface for prolonged periods, which is an advantage over single-agent sprays such as copper. Furthermore, chitosan provides physical and antimicrobial barriers; this contribution not only improves efficacy against pathogens but also reduces the amount of chemicals applied to the environment, promoting more sustainable agricultural practices.

Nanoemulsions offer clear advantages over conventional copper sprays under these sustained-release conditions. Copper salts depend on the formation of insoluble films that can be removed or degraded by rain and ultraviolet (UV) exposure. Furthermore, frequent applications and higher doses are required to maintain efficacy, increasing the risk of phytotoxicity and soil accumulation at levels that inhibit beneficial organisms [13,9]. According to Marin et al. [23], copper-based products widely used to control citrus canker may lead to the development of copper-resistant *Xanthomonas citri* subsp. citri. However, the same researchers indicated that a study on copper sensitivity in *X. citri* strains from the state of Paraná, Brazil, did not reveal the existence of resistant strains but rather copper-tolerant strains. In contrast, [18], reported the presence of copper-resistant Xanthomonas in Taiwan and its impact on the effectiveness of controlling these diseases using copper-based bactericides. The researchers reported that copper-resistant *Xanthomonas* isolates present two previously unreported variants of the copB gene, which differ from the other three types previously described in terms of size and structure. They concluded that there is a need to develop and include alternative measures instead of relying on foliar sprays of Cu-based bactericides. On the other hand, chitosan nanoemulsions incorporating GaOi can adhere tenaciously to the leaf cuticle thanks to chitosan's mucoadhesive properties, even in the presence of morning dew or light irrigation [32]. This adhesion, combined with the nanometric size of the droplets, ensures a uniform coating, minimizes potential runoff, and increases the persistence of the biocompound.

However, owing to their high stability, nanoemulsions allow them to be stored and transported without the need for rigorous conditions, thus establishing practical advantages for field applications. When applied directly to plants, these formulations present good adhesion to leaf surfaces, resistance to runoff, and washing away by rain, in addition to ensuring the controlled and prolonged release of active compounds [11]. The development of water-based nanoemulsions shows promising wide-range applications, whereas those formulated with chitosan have demonstrated additional potential owing to their ability to form a cohesive matrix that prevents degradation and promotes the retention of bioactive compounds.

In the field, the application of these nanoemulsions can be expanded to integrated disease management, which would complement agricultural practices such as crop rotation and the use of biological agents, resulting in a more resilient, efficient, and productive agricultural system. Therefore, the use of nanoemulsions transcends the benefits of this technology by offering a concrete and ecologically viable alternative for phytosanitary control. In this context, this study explores the development, properties, efficiency, and application possibilities for the control of *Xanthomonas citri* using water-based and chitosan nanoemulsions encapsulating gallate and eugenol as sustainable integrated high-impact systems. The main contribution of this study is the formulation of a novel oil phase (GaOi), in which hexyl gallate (0.5 % w/w) was stably solubilized in eugenol, enabling co-encapsulation and demonstrable potentiation of antimicrobial activity. Eugenol alone was bactericidal at 1.0 % (v/v), whereas GaOi-containing nanoemulsions achieved bactericidal effects at 0.03125 % (v/v) when formulated with chitosan (F64) and a bactericidal action of 0.125 % (v/v) when formulated with water (F24), both under identical REMA conditions. This observation strongly suggests a potentiating interaction between hexyl gallate and eugenol when they are co-formulated. The limitations of this study include the absence of formal quantitative synergy assays. Additional challenges for translation include the optimization of solubilization and emulsification parameters for scale-up.

2. Experimental

2.1. Materials

Nanoemulsions were prepared using chitosan (Qs) derived from crab shells, with 85 % degree of deacetylation and an average molecular weight of 190–310 kDa (Sigma Chemical Co.). Eugenol ($\geq$ 98 %), gallic acid, n-hexanol, and Tween 80 were purchased from Sigma-Aldrich (Brazil), and methanol (UV/HPLC grade) was obtained from Dinâmica (Indaiatuba, SP, Brazil). Deionized water with an electrical resistivity of 18 MΩ·cm was used in all formulations.

2.2. Synthesis of hexyl gallate

1-Hexanol (4 L) was heated to 80 °C and added 2.5 kg gallic acid slowly. The suspension was stirred at 120 °C for 15 min. Catalytic amounts of 65.29 g of p-toluenesulfonic acid (*p*-TosOH · H_2O) were added to the suspension and stirred at 165 °C. The progress of the reaction was monitored during 2 h by thin-layer chromatography (TLC). The mixture was neutralized to pH 6 with NaOH solution and cooled to 70 °C, and washed three times with 10 % brine solution. The reaction mixture was added in portions to petroleum ether 40-65 (2 vol), which was heated to 45 °C. After heating the reaction mixture to 55 °C, it was cooled to 5 °C at 0.05 °C/min while stirring. The suspension was filtered, and the solid crystals were washed twice with water and petroleum ether 40-65. The crystals were dried in vacuo at 70 °C, yielding hexyl gallate with a 75% yield.

2.3. Preparation of G6-loaded nanoemulsions

Before obtaining the nanoemulsions, it was necessary to dissolve G6 in the essential oil (0.5 g/100 g oil) due to its low solubility in polar media. The GaOi system was used as the oil phase in the emulsion production. Two processes were performed to obtain the emulsions: one using water as the continuous phase and the other using 1 g of chitosan/100 mL of solution, as shown in Table 1 (result section). A total of eight formulations were prepared, varying the GaOi concentration: four using water (GaOi-Water) as the continuous phase (F21–F24) and four using (GaOi-Qs) chitosan solution (F61–F64).

In the first process (formulations F21–F24), a mixture of deionized water with Tween 80 (at the same concentration of GaOi) was obtained, by stirring the surfactant (4500 rpm) until its complete incorporation. Afterwards, GaOi was added dropwise, at concentrations ranging from corresponding to 2 – 5 %, under high shear stirring (T25, IKA, Staufen, Germany) at 15000 rpm under cold bath for 5 min. In the second process (formulations F61–F64), 1 g Qs/ 100 mL was solubilized in 1 % acetic

Table 1
Antibacterial activity of formulations GaOi-Water (F21–24) and GaOi-Qs (F61–64) against *Xanthomonas citri* (FDC 02).

Formulations	GaOi concentration (%, v/v)	IC90 (%, v/v)	IC50 (%, v/v)	MBC (%, v/v)
21	2.0	0.082	0.040	0.50^{aA}
22	3.0	0.085	0.025	0.25^{bB}
23	4.0	0.026	0.008	0.125^{cC}
24	5.0	0.033	0.006	0.125^{cC}
61	0.10	0.029	0.026	0.03125^{aD}
62	0.25	0.029	0.027	0.03125^{aD}
63	0.50	0.031	0.027	0.03125^{aD}
64	0.75	0.029	0.026	0.03125^{aD}

IC90: minimum concentration for 90 % inhibition of bacterial growth. IC50: minimum concentration for 50 % inhibition of bacterial growth. MBC: minimum bactericidal concentration.
Means in the same column, with the same lower-case letter are not significantly different ($p < 0.05$), in relation to group formulation.
Means in the same column, for all groups, with the same capital letter are not significantly different ($p < 0.05$), in relation to all the formulations.

acid solution under constant mechanical stirring until complete dissolution. Subsequently, Tween 80 and GaOi were then added at the same equivalent concentrations calculated based on the dry mass of chitosan. Considering the chitosan concentration (10 mg/mL), GaOi levels ranged from 10 to 75 % of the chitosan dry mass. Tween 80 was incorporated by dripping under moderate agitation (4500 rpm), followed by the dropwise incorporation of GaOi, ensuring homogeneous distribution of the components. Emulsification was then performed at 15000 rpm for 5 min, using a cold bath to avoid thermal degradation of the constituents. The resulting emulsions were stored at 20 ºC protected from light to subsequent stability analysis.

2.4. Physicochemical characterization and stability of nanoemulsions

2.4.1. Determination of average droplet size, polydispersity and zeta potential

The mean diameter, polydispersity index (PDI), ζ potential, and size distribution of the samples were measured using dynamic light scattering (DLS) at 25 °C (ZetaSizer Nano S, Malvern Instruments, Worcester, UK) and a He-Ne laser at 627 nm with an incident angle of 90°. The zeta potential was measured after diluting the sample in deionized water at 2 % (v/v). It was calculated from electrophoretic mobility using the Helmholtz-Smoluchowski equation. Data analysis was performed using software provided with the equipment [39,5].

2.4.2. Atomic force microscopy (AFM)

Topographic images of the nanodroplets were obtained using AFM in triplicate. Initially, the nanoemulsion was dispersed in ultrapure water, and a small volume of the solution was deposited onto a freshly cleaved mica substrate. After deposition, the samples were dried at room temperature into a silica dissector to allow solvent evaporation and promote nanoparticle adhesion to the substrate. The dried samples were then analyzed using a Solver Next system (NT-MDT, Russia), operating in semi-contact mode at a scan frequency of 0.3 Hz.

2.4.3. Transmission electron microscopy (TEM)

The morphology and average size of the nanodroplets present in the nanoemulsions were evaluated by TEM, using a JEOL JEM-2100 LaB6 equipment operating at 200 kV. For sample preparation, the methodology of [21] was followed with modifications in which a small aliquot of the nanoemulsion, previously diluted in ultrapure water, was carefully dropped onto a copper grid coated with a carbon film (Formvar®). After deposition, the grids were kept at room temperature for natural drying and then stored under vacuum for 24 h, ensuring complete evaporation of the solvent before analysis. The particle size distribution was determined based on the measurement of approximately 200 individual droplets, using the ImageJ software (version 1.53q), allowing the calculation of the mean diameter and standard deviation.

2.4.4. Determination of efficiency of encapsulation by quantification of non-encapsulate eugenol

Hexyl gallate was dissolved in 0.5 % (w/w) eugenol, resulting in a single homogeneous oil phase, "GaOi." As hexyl gallate was completely solubilized in eugenol and its proportion in the oil phase was fixed, the encapsulation of the oil phase was determined by quantifying the free (unencapsulated) eugenol as an indirect marker. The free eugenol measured in the ultrafiltrate indicates the fraction of the oil phase present outside the nanoparticles; hexyl gallate is expected to be co-encapsulated with eugenol and not distributed independently to the aqueous phase under the conditions used.

The chitosan-based eugenol suspension was gently homogenized and subjected to ultrafiltration using Amicon® Ultra-15 centrifugal filter units (30 kDa, Millipore, Burlington, MA, USA) to separate nonencapsulated eugenol. The procedure was adapted from [14], with centrifugation performed at 4000 rpm for 30 min at 20 °C. The resulting filtrate, containing free eugenol, was then diluted in a methanol:ultrapure water mixture (70:30, v/v) for subsequent HPLC quantification.

Quantification of free eugenol was performed by high-performance liquid chromatography (HPLC) using a Waters ACQUITY Advanced Polymer Chromatography (APC) system equipped with an isocratic pump and a photodiode array detector (PDA). Chromatographic separation was carried out using an XBridge C18 column (3.5 µm, 4.6 × 50 mm; Waters Corporation, Milford, MA, USA) maintained at 40 °C. The mobile phase consisted of methanol and ultrapure water (70:30, v/v), delivered at a flow rate of 0.55 mL/min. The injection volume was 1 µL, and the autosampler was kept at 15 °C. UV detection was conducted at 280 nm with a spectral resolution of 3.6 nm. The total run time was 3 min under isocratic conditions. Quantification was based on an external calibration curve prepared in the same diluent, with concentrations ranging from 25.0 to 150.0 µg/mL.

Encapsulation efficiency (EE%) was calculated using the Eq. 1:

$$EE(\%) = \frac{WT - WNE}{WT} * 100\% \quad (1)$$

where WT is the total eugenol concentration in the suspension, and WNE is the concentration of free (non-encapsulated) eugenol measured in the filtrate. All measurements were carried out in triplicate, and the mean values were used for encapsulation efficiency calculations.

2.4.5. Bioactivity evaluation

To evaluate the concentration of nanoemulsions in the control of *Xanthomonas citri*, the Resazurin Plate Microtitration (REMA) technique was used, with some adaptations described by [38], to evaluate the inhibitory capacity of bioactives. 96-well microtiter plates were used for the tests, which were loaded at a reduced dose into subsequent wells in serial dilutions (1/2, 1/4, 1/8, 1/16, 1/32, 1/64, 1 /128) [4]. Bacteria were then inoculated into the wells at a concentration of 10^5 cells per well, standardized through CFU counting paired with OD measurement of inoculum (600 nm). Negative control (no compound), positive control (kanamycin at 20 µg/mL), and vehicle control were established using autoclaved deionized water at 50 % (v/v) concentration. The plates were then incubated for 16 h at 29 °C. An aliquot of resazurin (Sigma-Aldrich) was pipetted into each well to obtain a final concentration of 0.0015 %. After 1 h of reaction, the conversion of resazurin to resorufin, a fluorescent compound, was measured using a plate reader at 530 nm excitation and 590 nm emission wavelengths.

The change in color of the medium (blue to pink) indicated that there was a reduction of resazurin to resorufin in the presence of NADH (cell breathing), making it possible to determine the percentage of cells inhibited (IC) by the compound. The percentage of cell inhibition of the

treatments in relation to the negative control was calculated according to Eq. 1.

$$CI\ (\%)\ \frac{UAFc - UAFt}{UAFc} \quad . \quad 100 \qquad (2)$$

Where, CI (%) is the percentage of inhibited cells.

UAFc is the mean value of arbitrary fluorescence units in the negative control.

UAFt is the average value of arbitrary fluorescence units of the samples.

Using the dose-response graphs obtained, polynomial regression was applied to derive IC values in relation to the different concentrations of the tested compounds, as described by [29]. All tests were performed in triplicate, with three replicates for each compound in microtiter plates and three independent events.

2.4.6. Topical acute toxicity on the bees

Forager bees of the stingless bee's species Melipona scutellaris Latreille and Scaptotrigona postica (Latreille) (both Apidae: Meliponini) were collected from three different colonies maintained at the Meliponary of the Institute of Biosciences, UNESP, Rio Claro (São Paulo, Brazil). Colonies were healthy, free of disease and parasites, with actively laying queens to ensure sample representativeness. Sampling occurred on sunny days (>18 °C). Bees were placed in perforated plastic containers (250 mL; 5.7 × 9 × 7 cm) for ventilation. Subsequently, the bees were transported to the Ecotoxicology and Bee Conservation Laboratory, where they were maintained in climate-controlled chambers at 28 ± 1 °C and 80 ± 5 % of relative humidity (RH), both in complete darkness. Bees received sucrose solution (50 %) during a 2-hour acclimatization to reduce confinement stress.

The developed formulations were topically applied to assess their acute toxicity. Exposure was performed following OECD Guideline 214 by administering 1 μL of the test solution directly to the dorsal side of the prothorax using a Hamilton microsyringe. Each experimental unit consisted of ten bees confined to a single cage. Food consumption was measured using a 1.5 mL microcentrifuge tube filled with sucrose solution. As a positive control, a stock solution (0.10 ng/μL) of dimethoate (Dimexion® EC, 40 % of active ingredient, organophosphate, FMC Química do Brasil LTDA) was used, following the recommended guidelines for acute contact toxicity testing.

Bee mortality was recorded 24 h after exposure. The bioassays were conducted in a completely randomized design with three replicates per treatment under controlled environmental conditions (28 ± 1 °C, 80 ± 5 % RH, and darkness) [8].

2.4.7. Plant protection assays

A greenhouse experiment was conducted between February 20 and March 23, 2025, to evaluate the protective potential of formulations F24 and F64 in preventing the emergence of lesions caused by Xanthomonas citri, the etiological agent of citrus canker, as proposed by [44].

Citrus sinensis (L.) Osbeck nursery seedlings, cultivar 'Hamlin Sete Lagoas', grafted onto Swingle citrumelo rootstock (Citrus paradisi × Poncirus trifoliata), approximately 60 cm tall, were used in this study. The seedlings were transplanted into 7-liter plastic bags filled with a commercial pine-based substrate. The plants were maintained under an automated fertigation system using mineral fertilizer (Citrus 100, Amazon AgroSciences) at a rate of 200 mL per plant/day. The environmental conditions of the greenhouse such as temperature and relative humidity were continuously monitored using a digital thermo-hygrometer (HOBO MX2305), with hourly recordings. To ensure uniformity among the samples, branches containing young leaves at the V4 phenological stage (leaves approximately 4 cm wide and 10 cm long) were selected and marked, following the methodologies described by [6] and [44]. Five plants were used for each treatment, with at least three marked branches per plant. The nanoemulsions were applied by spraying until reaching the point of runoff. The bactericidal doses used for formulations F24 and F64 were standardized in function of REMA MBCs results, respectively. For comparison purposes, the positive control for infection consisted of the application of sterile saline solution (NaCl at 0.85 %, v/v), while the protection control was represented by the use of a commercial copper-based product (RECOP®, Albaugh Agro Brasil Ltda.) at the concentration recommended by the manufacturer (1.3 g/L in deionized water).

After 24 h of treatment application, all plants were inoculated with a bacterial suspension of X. citri, standardized to 10^8 cells/mL, diluted in saline solution. To promote infection, the plants were covered with transparent plastic bags for 24 h to ensure a humid and closed environment.

Approximately 30 days after inoculation, the marked leaves were collected and digitized using ImageJ software. The number of lesions was quantified and related to the leaf area (cm^2) using ImageJ Fiji software [35], allowing the density of lesions per leaf area to be obtained as a parameter of treatment efficacy.

2.5. Statistical analysis

Statistical Analysis of variance (ANOVA), calculation of the regression coefficient, and generation of three-dimensional surface graphs were performed using the Origin 2021 software. The significance of the equation parameters for each response was evaluated using the F-value at a probability of $p < 0.05$. Furthermore, the suitability of the models was determined through model analysis, a lack-of-fit test, and coefficient of determination (R^2) analysis. All measurements were performed in triplicate, and the results are reported as means and standard deviations of the analyses.

Topical acute toxicity in bees was evaluated through the application of a binomial generalizad linear model. Goodness of fit was assessed with the 'hnp' package [28], and contrasts were performed via the 'glht' function from the multcomp package [12]. Analyses were conducted in RStudio 4.3.2 [40]. For data presentation, mortality is expressed as percentages with 95 % binomial confidence intervals (Wilson method), which restrict estimates to the biologically significant range (0–100 %).

Regarding food consumption data were tested for normality and homoscedasticity using Shapiro-Wilk and Bartlett tests. As assumptions were not met, a Kruskal–Wallis test with Dunn's post hoc ($p < 0.05$) was performed using agricolae package [24].

For the plant protection assays, the GraphPad Prism v.6 software (GraphPad Software, San Diego, CA, USA) was used. Considering the nature of the data, the nonparametric Kruskal-Wallis test was applied, followed by the Dunn post-hoc test, with a significance level of $p \leq 0.05$ and three degrees of freedom, to identify statistical differences between treatments.

3. Results and discussion

3.1. Production and average size of nanoemulsions

The identification of hexyl gallate used in the formulations was confirmed by ^1H and ^{13}C NMR (Supplementary Fig 1). The main resonances (400 MHz, DMSO-d6) observed include singlets at δ 9.24 (2 H) and 8.92 (1 H), attributable to the three phenolic OH protons of the 3,4,5-trihydroxybenzoate portion; an aromatic singlet at δ 6.94 (2 H) consistent with the two equivalent protons of the ring (H-2 and H-6); and the methylene OCH_2 group of the ester at δ 4.15 (t, $J = 6.5$ Hz, 2 H). The remaining aliphatic resonances appear as multiplets between δ 1.70–0.79 and correspond to the hexyl chain (–CH_2– and terminal CH_3). On the other hand, the ^{13}C spectrum shows the expected carbonyl carbon at δ 165.9 and signs of aromatic carbon at δ 145.6, 138.4, 119.6, and 108.5; the oxygenated methylene resonates at δ 63.99, while the aliphatic carbons of the hexyl chain appear at δ 30.9, 28.3, 25.2, 22.1, and 13.9 [34,4].

The nanoemulsions produced with water as the continuous phase demonstrated excellent stability over 30 days of storage, indicating their robustness. The use of GaOi (essential oil and gallate) concentrations ranging from 2 to 5 % (Table 1), allowed the systematic evaluation of the impact of the amount of the oil phase on the physicochemical characteristics and stability of the nanoemulsions. The average droplet size of the nanoemulsions was consistently maintained within the range of 140 – 223 nm. This range is suitable to enhance the biological interactions due to the high surface area available [25]. Additionally, polydispersity index (PDI) values below 0.5 indicate a narrow droplet size distribution, reflecting the efficiency of the emulsification process and kinetic stability. Another critical parameter for assessing the stability of the nanoemulsions was the zeta potential, whose negative values greater than −14 mV suggested the presence of sufficient electrostatic repulsion to prevent droplet coalescence. This repulsion stabilizes the nanoemulsions, reducing their tendency for aggregation and flocculation, which could compromise their integrity over time. The stability observed at all GaOi concentrations reinforces the efficiency of Tween 80 as an emulsifier, promoting a homogeneous dispersion of the essential oil in the aqueous matrix.

The nanoemulsions formulated using chitosan solution as aqueous phase also showed stability for over 60 days of storage, demonstrating the efficiency of the system in maintaining its structural properties over time. This group used GaOi concentrations ranging from 10 to 75 % based on the dry mass of the polymer (Table 1). The average droplet size ranged from 388.3 to 496.6 nm, indicating the formation of submicron-scale structures. These sizes were larger than those of GaOi-Water, which can be attributed to the higher viscosity of the chitosan solution, resulting in larger droplets [33]. PDI value of for GaOi-Qs was lower than 0.54, indicating a relatively homogeneous distribution of droplet sizes. Although this value was higher than that found in GaOi-water (PDI $<$ 0.5), it was still within the range considered acceptable for stable colloidal system [27]. The zeta potential, with values above + 52 mV, reflects the contribution of chitosan, a cationic polymer that adsorbs on the surface of the droplets, providing stability to the system through electrostatic repulsion interactions among droplets [19]. These values indicate an efficient energy barrier against coalescence, which ensures the integrity of the nanodroplets over time. The differences in the average sizes and zeta potentials reflect the distinct stabilization mechanisms between the formulations. In GaOi-Water, Tween 80 alone was responsible to promote stabilization by adsorption on the interface of the oil droplets, whereas in GaOi-Qs, chitosan contributed to cationic stabilization, forming a protective layer around them. In addition, the higher viscosity of the chitosan solution in GaOi-Qs directly influences the size of the droplets because the more viscous fluids, the more difficult to break the oil phase into smaller droplets during emulsification. Despite these differences, both systems demonstrated good stability over time, indicating the efficiency of the components used. However, their intrinsic characteristics render these systems suitable for different applications. Smaller nanoemulsions (GaOi-Water) are preferable for formulations in which the visual appearance is critical. Larger nanoemulsions with higher zeta potential (GaOi-Qs) may be more suitable for antimicrobial applications, such as *Xanthomonas citri*. Fig. 1 presents a schematic representation of formulation 64, illustrating the complete solubilization of hexyl gallate in eugenol to form the GaOi oil phase, followed by the formation of the nanoemulsions. The figure highlights the role of Tween 80 as a non-ionic surfactant that promotes the interfacial stabilization of oil droplets and, in chitosan-based systems, the stabilization of oil droplets. This scheme supports the previously discussed physicochemical interpretations regarding the droplet size, surface charge, and stability of the GaOi-water and GaOi-Qs nanoemulsions.

3.2. *Morphology characterization of the water- and chitosan-based emulsions*

The AFM micrographs in Fig. 2 show that both the water-based and chitosan-based emulsions exhibit spherical and well-dispersed structures, confirming the efficiency of the eugenol encapsulation system in the aqueous medium. In the emulsion F21 (Fig. 2a), formulated with 2 % (v/v) of eugenol, droplets with diameters ranging from 40 to 90 nm were observed, values perfectly compatible with the average size of 109 nm obtained by DLS. In the emulsion F24 (Fig. 2b), with a higher eugenol content (5 %, v/v), droplet sizes ranged from 50 to 150 nm, reflecting the higher amount of the oil phase. Despite the broader size distribution, the AFM results matched the DLS data and confirmed the system's uniformity and stability, even under higher oil loading. Similar results were obtained by [43]. Nanoemulsions were produced using various essential oils, including eugenol (O/W), and exhibited slightly smaller droplet sizes than those recorded in the present study, possibly as a consequence of the nanoparticle formation method and processing time (high-speed ultrasonic homogenization at 15000 rpm for 20 min). Thus, the researchers concluded that nanoemulsions were more efficient in controlling microorganisms owing to their increased solubility compared with free-form essential oils. Therefore, such nanometric morphological characteristics are extremely promising for controlling

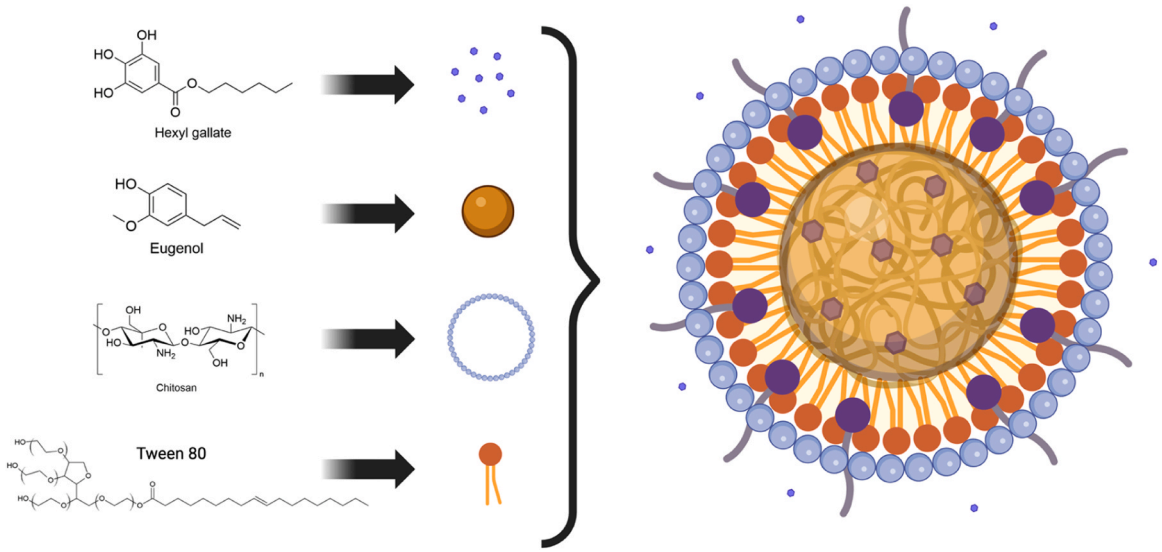


Fig. 1. Schematic representation of GaOi-Qs-based nanoemulsions.

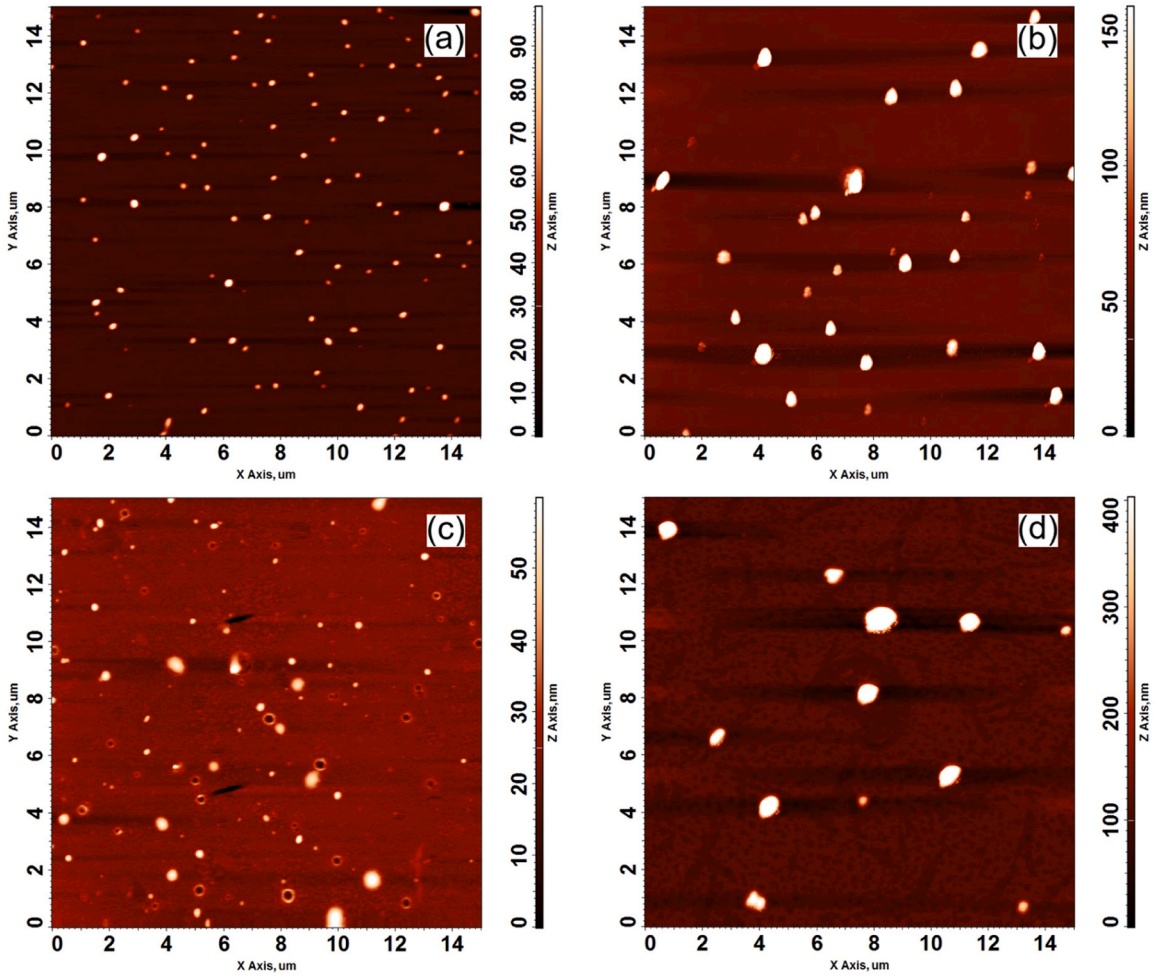


Fig. 2. AFM images 2D for F21 (a), F24 (b), F61 (c), F64 (d).

X. citri. This is because droplets in the nanometric fraction have a larger contact area and consequently a greater potential for penetration into the bacterial cell wall, thus ensuring the rapid and effective action of GaOi. In contrast, larger droplets, up to 150 nm, in water-based emulsions facilitate the transport of a greater quantity of the active ingredient, which is advantageous for controlling microorganisms, as indicated by the MBC of 0.125 % (F24). Therefore, in practical applications, a smaller quantity of emulsion 24 was necessary to ensure a continuous protective barrier on citrus leaves.

The micrographs of the chitosan-based emulsions confirmed the formation of spherical and uniformly distributed droplets, with dimensions that varied according to the eugenol load. In emulsion F61 (Fig. 2c with 0.10 % (v/v) of eugenol), droplets ranged between 20 and 50 nm, though DLS reported an average diameter of 388 nm. This difference was due to the dilution of the sample before deposition on mica, which favors the visualization of the less aggregated and more stable fractions. In addition, the high zeta potential of + 53.85 mV corroborated the excellent dispersion and electrostatic stability, avoiding coalescence even at low eugenol concentrations.

In contrast, emulsion F64 (Fig. 2d; 0.75 % (v/v) of eugenol) presented droplets with diameters exceeding 400 nm, consistent with DLS and zeta potential results. This size increase reflects the greater fraction of the retained oil phase; however, the polymeric matrix continues to ensure a homogeneous dispersion and resistance to sedimentation. Similar results were reported by [10], who observed a 48.2 % size increase with an 80 % rise in eugenol content at a 1:1 chitosan:eugenol ratio.

Therefore, the smaller droplets observed in emulsion F61 provide a larger interfacial area, which may facilitate a more efficient interaction between the oil phase and *Xanthomonas citri* membrane, potentially increasing the biocidal effect of eugenol. In contrast, the larger droplets in emulsion F64 may provide a greater mass of eugenol per droplet, thus contributing to a more persistent coverage on the leaf surface, which may favor prolonged preventive activity. The higher apparent viscosity conferred by chitosan likely influenced the particle size by increasing the shear strength during homogenization, producing larger droplets. In addition, chitosan exhibits intrinsic bactericidal properties and, given its cationic character ($\zeta > +50$ mV), may interact electrostatically with anionic bacterial membranes, producing a possible synergistic effect with eugenol. Cruz et al. [7], compared the efficiency of several nanoemulsions with different oils and reported against *X. citri* an MBC > 0.5 % for O/W eugenol-based nanoemulsions. In contrast, in the present study, an MBC of 0.125 % was found for water-based and 0.03125 % for chitosan-based, demonstrating the potential synergistic effect of the polymer in controlling the pathogen. However, the claim of prolonged action is an inference drawn from formulation properties.

Morphological characterization of the emulsions was also performed using TEM, enabling direct analysis of the structure and distribution of the nanodroplets. Fig. 3a shows the microscopy of formulation F24, in which the presence of spherical structures, well individualized and dispersed throughout the micrograph could be observed. This morphology was consistent with the data previously obtained by DLS and AFM, reinforcing the consistency and stability of the developed colloidal system. Although some regions revealed particle groupings, these agglomerates were likely the result of the sample preparation process for analysis such as drying or interaction with the support.

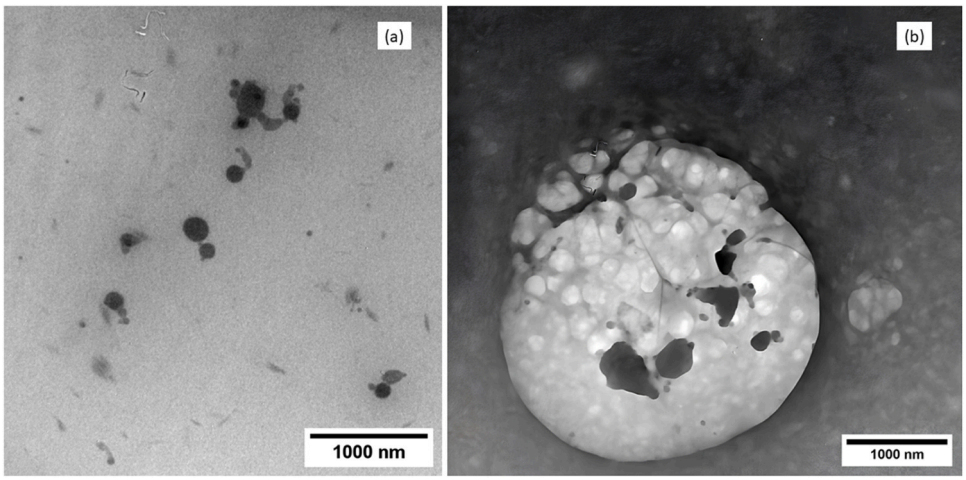


Fig. 3. TEM images for F24 (a) and F64.

Nevertheless, the general dispersion of the droplets suggests adequate stability of the system and the ability to maintain droplet integrity during analysis. In contrast, emulsion F64 (Fig. 3b) exhibited a more complex structural profile, characterized by larger agglomerates composed of smaller internal nanodroplets. This organization can be attributed to the high viscosity of the chitosan polymer matrix, which contributes to the formation of denser and shear-resistant structures. The visualization of encapsulated nanodroplets within an aggregated matrix reinforces the hypothesis of efficient encapsulation of the essential oil, which may be advantageous for controlled release systems [1].

Therefore, it is important to highlight that, in both formulations, the nanodroplets exhibited a defined spherical morphology, indicating the efficiency of the encapsulation process, in addition to the physicochemical stability, which are crucial factors for the biological performance of the formulation [10]. In this sense, the micrographs corroborate the data obtained in the analysis of cell viability by the REMA assay, in which the nanoemulsions demonstrated superior action to copper sulfate in the control of *Xanthomonas citri*. The presence of spherical and well-distributed nanodroplets, associated with the efficient encapsulation of eugenol, gives the system greater efficiency for the transport and possible controlled release of the active compound to ensure phytosanitary control.

The chitosan-based nanoemulsion developed in this study achieved an encapsulation efficiency (EE %) of 82.8 ± 0.6 %, a value determined by ultrafiltration, which infers the selective retention of charged droplets followed by quantification by HPLC. The carrier system developed in this study presents high performance when compared to that reported in the literature, where [42] presented an EE % of only 2.36 – 20.17 % in chitosan nanodroplets containing eugenol obtained by ionic gelation. Shao et al., [36] reached a maximum of 11.61 % using ultrasonic emulsification. Thungphotrakul, Prapainainar [41] observed an EE % of 69.96 – 98.04 % when encapsulating clove essential oil (predominantly eugenol) in chitosan, reinforcing the direct relevance of the comparison.

The high EE % obtained in this study may be due to the combination of the analytical and formulation factors. First, the inclusion of hexyl gallate in eugenol to form the oily phase could enhance hydrophobic interactions with the polymeric tail of chitosan, forming a more cohesive core that retains the active ingredient more effectively [17]. Second, the adopted analytical methodology of prior ultrafiltration and high-resolution HPLC surpasses conventional methods based solely on centrifugation and UV-Vis spectroscopy in terms of selectivity, allowing for the precise discrimination of free and encapsulated eugenol fractions. Therefore, a high EE % indicates a greater load of active ingredients per nanoparticle, possible controlled release, and minimization of losses due to early diffusion or coalescence. Consequently, these characteristics are essential in agricultural applications, as they ensure the delivery of the antimicrobial compound in a controlled manner, prolonging its efficacy in the field and reducing the need for reapplication. Thus, these considerations reinforce the importance of both formulation design and methodological rigor in achieving high encapsulation efficiency and generating comparable and reliable data.

The results of Viability tests (REMA) indicated that very low concentrations of the water-based emulsion formulation could significantly reduce microbial viability (Table 1). Therefore, it was clear that a minimum bactericidal concentration (MBC) of 0.125 % (v/v) presents an efficient bactericidal profile against *Xanthomonas citri* for the emulsions F21–24 (Fig. 4). On the other hand, the formulations (F61–64) containing chitosan as an additional component demonstrated superior performance compared to the water-based formulations. Formulation F64, with IC50 and IC90 values of 0.026 % and 0.029 % (v/v), respectively, and an MBC of only 0.03125 % (v/v), indicated a more efficient microorganism control power (Fig. 5). Thus, the improved performance could be attributed to the intrinsic bioactive properties of chitosan, which include its ability to interact with bacterial membranes, promote destabilization, and increase cell permeability. Therefore, the synergistic action between chitosan and the active compounds enhanced the antimicrobial effect, allowing similar efficacy to be achieved at

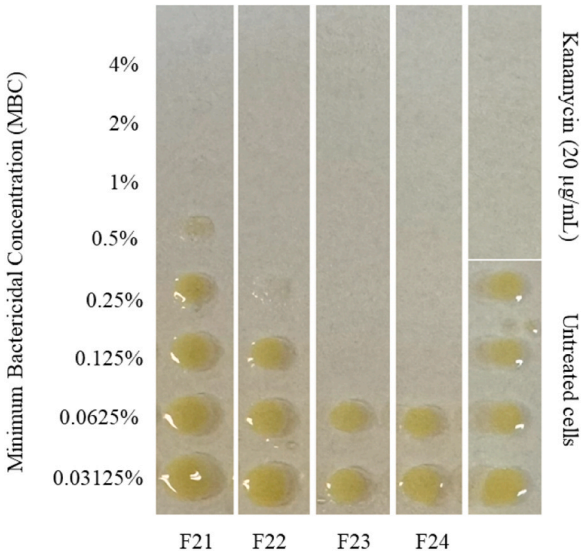


Fig. 4. Bactericidal effects of nanoemulsions F21-F24 against *X. citri*.

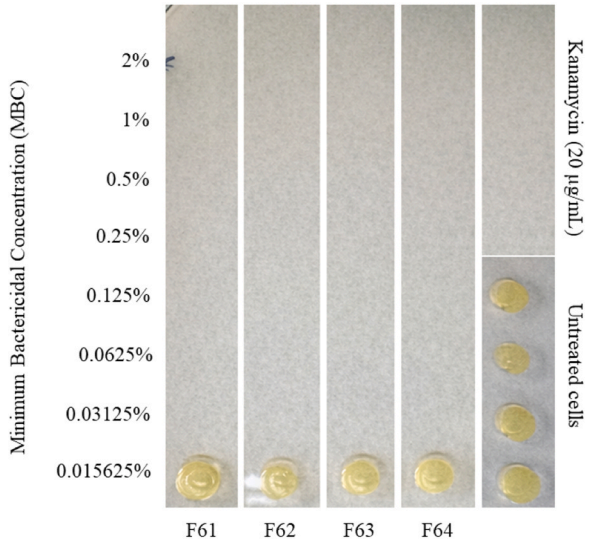


Fig. 5. Bactericidal effects of nanoemulsions F61-F64 against *X. citri*.

significantly lower concentrations. It is worth noting that the superiority of chitosan-based emulsions is relevant in terms of practical applications because of their bactericidal effect at lower concentrations, thus reducing the amount of material required for use in the field or in industrial formulations. Therefore, there is high economic viability, in addition to minimizing the environmental impact.

3.3. Topical acute toxicity on the bees

The acute toxicity bioassays (Table 2) demonstrated that nanoemulsions F24 and F64 were completely harmless to the forager bees *M. scutellaris* and *S. postica*, exhibiting survival and feeding profiles equivalent to or superior to those of the negative control (water).

In *M. scutellaris*, the positive control (dimethoate) caused 100 % mortality in 24 h, confirming the sensitivity of the assay and the high toxicity of the organophosphate. In contrast, formulations F24 and F64 caused only 3.3 % and 0 % mortality, respectively, which was statistically equivalent to that observed in the water control (3.3 %). Food consumption revealed that, while dimethoate drastically reduced intake (5.9 mg/bee), bees exposed to F24 and F64 consumed an average of 51.6 mg and 46.2 mg of sucrose solution per individual, respectively, values significantly higher than the water control (29 mg), which indicates not only the absence of an antifeedant effect but even a slight stimulation of consumption.

Furthermore, to verify whether the observed safety and acceptability patterns are maintained in other species of native bees, the same treatments were evaluated in *S. postica*, a species that presents distinct physiological and behavioral characteristics. In this species, none of the treatments caused mortality (0 % in water, F24, and F64), whereas dimethoate again led to 100 % mortality. Consumption between treatments did not differ statistically (7.5 mg in dimethoate, 8.7 mg in F24, 13.9 mg in F64, and 9.8 mg in the water control). Therefore, it is suggested that this species presents a lower behavioral sensitivity to the compounds tested but mainly that the formulations did not interfere with the normal feeding pattern.

Similar results were reported by [15], who highlighted that clove oil, with eugenol content between 50 % and 87 %, was not harmful to *Apis mellifera* L. (Apidae: Apini), causing only 3 % mortality. In addition, the researchers emphasized the selective efficacy of eugenol, achieving 100 % lethality in the parasite mite *Varroa destructor* (Acari: Varroidae) after 48 h of exposure, reinforcing the potential of this compound as a pest control agent without compromising pollinators. The safety demonstrated by formulations F24 and F64 was consistent with the literature, indicating that chitosan and eugenol are agents of low toxicity to pollinators, especially when adequately encapsulated [26,3].

The slight increase in consumption observed in *M. scutellaris* can be inferred as a slight attraction of the bee to the compounds or taste of eugenol, as discussed by [3], without compromising its health or longevity. In addition, the lack of mortality and maintenance of food intake suggest that the nanodroplets are sufficiently stable, as previously discussed, and do not disintegrate into potentially toxic compounds during cuticular contact.

Table 2
Mortality (%) and food consumption of stingless bees exposed to effective nanoemulsions for *Xanthomonas citri*.

Treatment	*Melipona scutellaris*		*Scaptotrigona postica*	
	*Mortality (%)	**Food consumed (mg/bee)	*Mortality (%)	**Food consumed (mg/bee)
Water	3.33 (0.00 – 18.00)^{a}	28.97 ± 12.44^{ab}	0.00 (0.00–0.00)^{a}	9.81 ± 1.00^{a}
Dimethoate	100 (100 – 100)^{b}	5.93 ± 3.69^{b}	100 (100–100)^{b}	7.51 ± 1.23^{a}
F 24	3.33 (0.00 – 18.00)^{a}	51.58 ± 5.52^{a}	0.00 (0.00–0.00)^{a}	8.74 ± 0.30^{a}
F 64	0.00 (0.00 – 0.00)^{a}	46.15 ± 4.62^{a}	0.00 (0.00–0.00)^{a}	13.93 ± 4.30^{a}

* Means and confidence intervals followed by the same lowercase letter are not significantly different according to contrasts from the binomial generalized linear model ($p < 0.05$). ** Means ± standard error (n = 30) followed by the same letter within columns are not significantly different according to Dunn's test with Bonferroni correction ($p < 0.05$).

3.4. Plant protection assays

The greenhouse assays were conducted under controlled environmental conditions, with temperature and relative humidity maintained within a constant operating range throughout the assay (Fig. 6). Stability of environmental conditions is crucial to minimize abiotic stress on plants and pathogens, thus ensuring that differences in lesion development truly reflect the efficacy of the treatments, rather than microclimate fluctuations. The formulations were tested as a function of the concentrations derived from the REMA results (MBCs). F24 at 0.125 % (v/v) and F64 at 0.03125 % (v/v) against *Xanthomonas citri* on 'Hamlin Sete Lagoas' orange trees.

Formulation F24 (Fig. 7a) was evaluated in comparison with the standard copper treatment (RECOP® at 1.3 g/L). In untreated plants, the leaves developed an average of 2.58 lesions cm^{-2} (SD = 1.56) per leaf area. Copper application reduced lesion density to 0.26 cm^{-2} (SD = 0.23), corresponding to a 92.3 % reduction ($p \leq 0.05$ vs. control). Notably, formulation F24 (Fig. 7b) achieved 0.53 lesions cm^{-2} (SD = 0.38), a 79.5 % reduction ($p \leq 0.05$ vs. control), and did not differ significantly from copper spraying ($p \leq 0.05$).

In the same assay, positive-control leaves developed an average of 2.54 lesions cm^{-2} (SD = 1.47). Treatment with copper (RECOP®, 1.3 g/L) reduced lesion density to 0.52 cm^{-2} (SD = 0.38), corresponding to a 79.4 % reduction versus control ($p < 0.05$). Likewise, the F64 nanoemulsion (Fig. 7c,d) lowered lesion density to 0.66 cm^{-2} (SD = 0.48), a 74.0 % reduction compared to control ($p < 0.05$) and not significantly different from copper ($p > 0.05$).

These results demonstrate that even without a polymeric matrix, F24 can ensure broad leaf coverage and rapid interaction with *Xanthomonas citri*, thereby inhibiting lesion development. Similar studies on essential oils in aqueous emulsions have also reported substantial protection against phytopathogens [44]. Furthermore, the performance of F64 demonstrated that even when applying a very low concentration, the chitosan matrix may promote the controlled release of GaOi, thus maintaining prolonged protective activity, similar to the barrier formed by copper salts [22]. Studies on polymeric nanoemulsions have shown

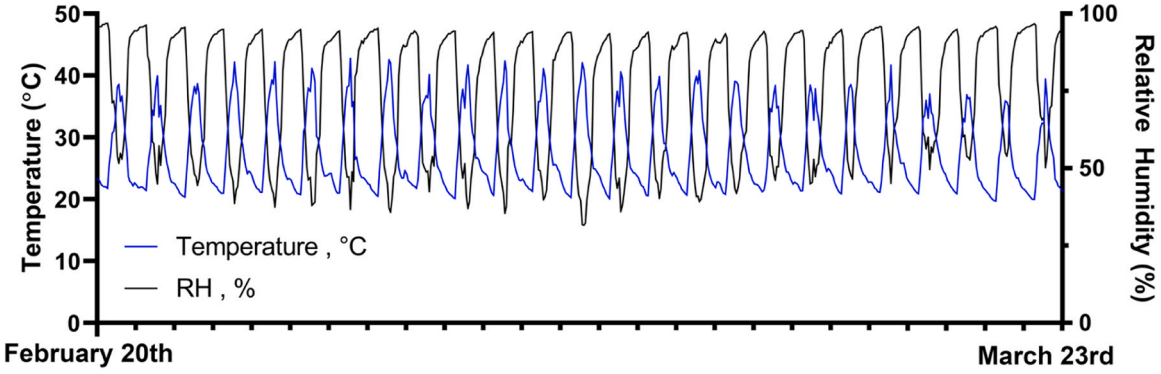


Fig. 6. Temperature and relative humidity operating range throughout the assay.

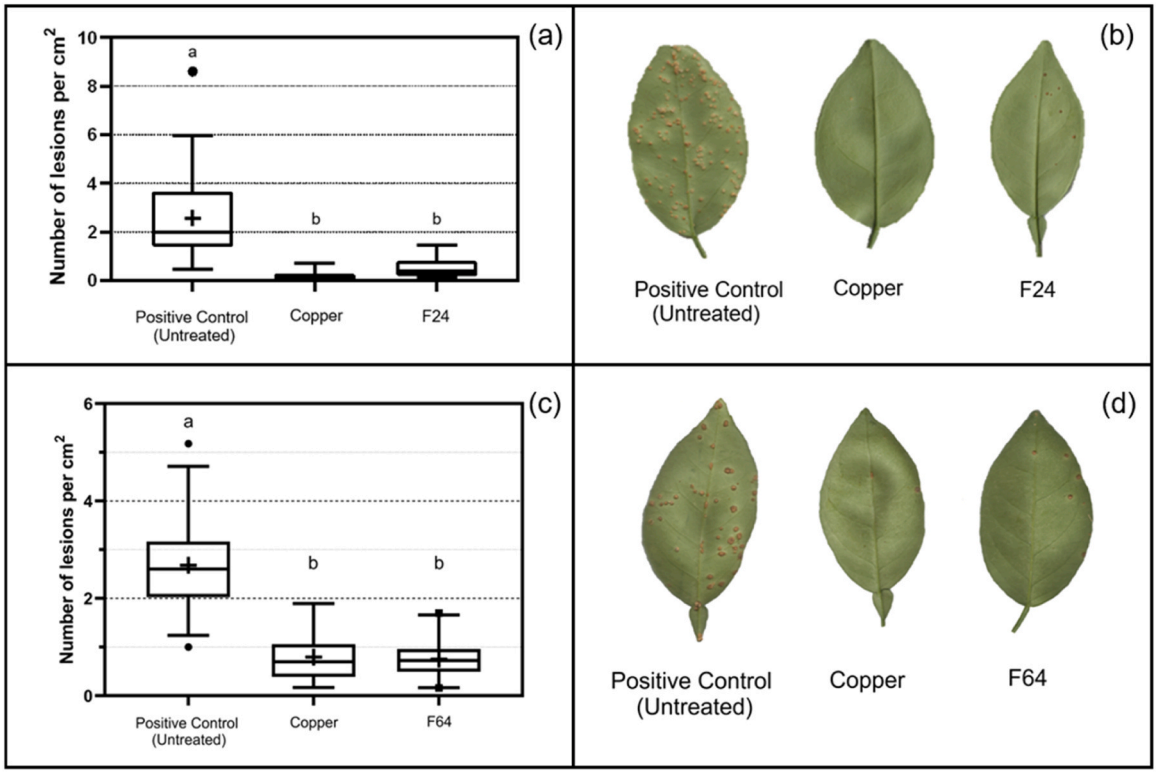


Fig. 7. Efficacy of nanoemulsions F24 and F64 versus copper in reducing citrus canker lesions under greenhouse conditions. Box-and-whisker plot showing lesion density of F24 (a), Representative digital scans of leaves from F24 treatment (b), Box-and-whisker plot showing lesion density of F64 (c) and Representative digital scans of leaves from F64 treatment (d). Lowercase letters indicate groups statistically similar ($p \geq 0.05$) according to the nonparametric Kruskal-Wallis test, followed by the Dunn post-hoc test. Statistical analysis was performed in GraphPad Prism software (v. 6.0).

that this encapsulation strategy prolongs the antimicrobial effect and improves adhesion to leaf tissues [16,20]. Therefore, F64 has an efficacy comparable to that of copper, with a possible controlled release profile.

Although the two treatments significantly reduced canker lesions, they may offer different release profiles. This is because F24 generates immediate action and broad coverage, whereas F64 could ensure controlled release and leaf mucoadhesion. These results were consistent with those reported in the literature on the development of nanoemulsions with eugenol and G6 as analytes as promising alternatives to traditional chemical control, combining efficacy and reducing the risks of phytotoxicity and accumulation of metals in the soil, in addition to offering a more environmentally sustainable alternative [16,3,44].

4. Conclusion

Synthesized nanoemulsions are of interest for industrial applications because the particle size provides a larger surface area, which could favor the controlled release of active compounds such as GaOi. The moderate electrostatic stability of GaOi-Water formulations (water as a continuous matrix), conferred by the negative zeta potential ($\zeta \approx < -14$ mV), suggests good resistance to flocculation under industrial conditions. GaOi-Water nanoemulsions have demonstrated promising performance owing to their simpler and lower-cost composition compared to GaOi-Qs nanoemulsions. showed a lesion reduction efficiency of 79.46 % compared to the positive control, and F24 was statistically equivalent to conventional copper treatment, reinforcing its potential as a sustainable alternative. In addition, it exhibited structural stability, integrity, and antimicrobial activity over prolonged periods.

In contrast, nanoemulsion based on chitosan presented attributes that indicate significant potential for antimicrobial applications, as evidenced by the REMA results. In addition, this formulation is particularly interesting for use in conditions where durability and interaction with surfaces or solid matrices are critical, such as in open-field applications. Smaller nanoemulsions with a high surface area and potential for penetration into plant tissues are ideal for foliar spray applications. Rapid dispersion and adhesion to leaf surfaces, combined with the possible gradual release of GaOi, increased the effectiveness of *Xanthomonas citri*. control, ensuring prolonged action. Furthermore, the nanoemulsions based on chitosan offer dual action. First, they act as direct antimicrobial agents against *Xanthomonas* owing to their ability to interact with the bacterial cell membrane. In addition, the high zeta potential confers stability to nanoemulsions in solutions with a higher nutrient load or organic residues, which is typical of the agricultural environment.

CRediT authorship contribution statement

Jaiber Humberto Rodriguez Llanos: Writing – original draft, Methodology, Investigation, Formal analysis, Conceptualization. **Eddyn Gabriel Solorzano Chavez:** Writing – review & editing, Methodology, Investigation, Formal analysis. **Danieli Fernanda Canaver Marin:** Writing – review & editing, Methodology, Formal analysis. **Rayane Monique Sete da Cruz:** Writing – review & editing, Methodology, Formal analysis. **Vitor Rodrigues Marin:** Writing – review & editing, Methodology, Formal analysis. **Caio Felipe Cavicchia Zamuner:** Writing – review & editing, Methodology, Formal analysis. **Terezija Jovanovski:** Writing – review & editing, Methodology, Formal analysis. **Geovanny Barroso:** Writing – review & editing, Validation, Methodology, Formal analysis. **Osmar Malaspina:** Writing – review & editing, Supervision, Resources, Data curation. **Peter J. Deuss:** Writing – review & editing, Supervision, Resources, Data curation. **Dirk-Jan Scheffers:** Writing – review & editing, Supervision, Resources, Data curation. **Henrique Ferreira:** Writing – review & editing, Supervision, Resources, Data curation. **Michel Brienzo:** Writing – review & editing, Supervision, Project administration, Funding acquisition, Conceptualization.

Animal experiment statement

The experiments conducted in this study involved only stingless bees (Hymenoptera: Apidae: Meliponini), which are invertebrates. According to Brazilian legislation (Law No. 11.794/2008) and the guidelines of the National Council for the Control of Animal Experimentation (CONCEA), ethical approval is required exclusively for research involving vertebrate animals. Therefore, no ethics committee approval was necessary for the experimental procedures described herein. All handling of bees followed relevant national regulations and best practices for the care and welfare of invertebrates used for scientific purposes. Authorization Sisgen – 15754, registration A21B2E5.

Declaration of Competing Interest

There are no conflicts of interest to declare.

Acknowledgments

This research was supported by Netherlands Organization for Scientific Research (NWO - Netherlands) and (São Paulo Research Foundation (FAPESP - Brazil) under grant 2023/12187–0; 2023/06702–9; 2021/10839–4; 2024/06991–3, and Brazilian National Council for Scientific and Technological Development (grant number 305078/2025–9; 403481/2025–2; 304138/2023–1). AP is thankful for the financial support from Deutsche Forschungsgemeinschaft (DFG, German Research Foundation) – project 525894115 within the Priority Program SPP 2416 "Codeχ – The code of chito-protein interactions" and financial support from Federal Ministry of Food and Agriculture (BMEL) based on a decision of the parliament of the Federal Republic of Germany via the Federal Office for Agriculture and Food (BLE) under the Federal Programme for Ecological Farming. The authors thank the Biobased Chemistry & Refinery group at the Hanze University of Applied Science for upscaling the synthesis of hexyl gallate (G6).

Appendix A. Supporting information

Supplementary data associated with this article can be found in the online version at doi:10.1016/j.apmt.2026.103191.

Data availability

Data will be made available on request.

References

[1] T. Anand, M. Anbukkarasi, P.A. Thomas, P. Geraldine, A comparison between plain eugenol and eugenol-loaded chitosan nanoparticles for prevention of in vitro selenite-induced cataractogenesis, J. Drug Deliv. Sci. Technol. 65 (2021) 102696, https://doi.org/10.1016/J.JDDST.2021.102696.

[2] J.M.H.F. Barros, A.A. Santos, M.J. Stadnik, C. da Costa, Comparison of nanoemulsions prepared with cinnamon, eucalyptus, mountain pepper, and Palmarosa essential oils for antifungal application, Bionanoscience 15 (2025) 1–14, https://doi.org/10.1007/S12668-024-01650-3/FIGURES/6.

[3] J. Caren, Y.C. Zhu, Q.D. Read, Y. Du, Risk assessment of effects of essential oils on honey bees (Apis mellifera L.), Insects 16 (2025) 303, https://doi.org/10.3390/INSECTS16030303/S1.

[4] L.B. Cavalca, C.F.C. Zamuner, L.L. Saldanha, C.R. Polaquini, L.O. Regasini, F. Behlau, H. Ferreira, Hexyl gallate for the control of citrus canker caused by Xanthomonas citri subsp citri, Microbiologyopen 9 (2020) e1104, https://doi.org/10.1002/MBO3.1104.

[5] M.A. Chaves, L. Baldino, S.C. Pinho, E. Reverchon, Co-encapsulation of curcumin and vitamin D3 in mixed phospholipid nanoliposomes using a continuous supercritical CO_2 assisted process, J. Taiwan Inst. Chem. Eng. 132 (2022) 104120, https://doi.org/10.1016/J.JTICE.2021.10.020.

[6] J.C. Cifuentes-Arenas, A. de Goes, M.P. de Miranda, G.A.C. Beattie, S.A. Lopes, Citrus flush shoot ontogeny modulates biotic potential of Diaphorina citri, PLoS One 13 (2018) e019056363, https://doi.org/10.1371/JOURNAL.PONE.0190563.

[7] G. Cruz, J. GolÇalves De Oliveira Filho, M. De Mori, M. Ribeiro, C.W. Oliveira De Souza, M.D. Ferreira, Antibacterial activity of nanoemulsions based on essential oils compounds against species of Xanthomonas that cause citrus canker, Biointerface Res. Appl. Chem. 12 (2022) 1835–1846, https://doi.org/10.33263/BRIAC122.18351846.

[8] I.M. da Silva, J.C. Zanuncio, B.P. BrÜgger, M.A. Soares, A.J.V. Zanuncio, C. F. Wilcken, W. de S. Tavares, J.E. SerrAo, C.S. Sediyama, Selectivity of the botanical compounds to the pollinators Apis mellifera and Trigona hyalinata (Hymenoptera: Apidae), Sci. Rep. 10 (2020), https://doi.org/10.1038/S41598-020-61469-2.

[9] T.T. Dao, T.T.T. Tran, A.M. Nguyen, L.N. Nguyen, P.T.M. Pham, T. Tsubota, M. N. Nguyen, Fungicide application can intensify clay aggregation and exacerbate copper accumulation in citrus soils, Environ. Pollut. 288 (2021) 117703, https://doi.org/10.1016/J.ENVPOL.2021.117703.

[10] S. Das, V.K. Singh, A.K. Dwivedy, A.K. Chaudhari, Dubey, N.K. Deepika, Eugenol loaded chitosan nanoemulsion for food protection and inhibition of Aflatoxin B1 synthesizing genes based on molecular docking, Carbohydr. Polym. 255 (2021) 117339, https://doi.org/10.1016/J.CARBPOL.2020.117339.

[11] S. Dhanasekaran, L. Liang, S. Gurusamy, Q. Yang, H. Zhang, Chitosan stabilized lemon essential oil nanoemulsion controls black mold rot and maintains quality of table grapes, Int. J. Biol. Macromol 277 (2024) 134251, https://doi.org/10.1016/J.IJBIOMAC.2024.134251.

[12] Dinno, A., 2025. Title Dunn's Test of Multiple Comparisons Using Rank Sums. cran.r-project.org.

[13] S.F. El-Gioushy, R. Sami, A.A.M. Al-Mushhin, H.M. Abou El-Ghit, M.S. Gawish, K. A. Ismail, R.M.Y. Zewail, Foliar application of ZnSO4 and CuSO4 affects the growth, productivity, and fruit quality of Washington Navel Orange Trees (Citrus sinensis L.) Osbeck, Horticulturae 7 (2021) 233, https://doi.org/10.3390/HORTICULTURAE7080233.

[14] L.S. Ferreira, B.B. da Silva, M.A. Chaves, S.C. Pinho, Physicochemical characterization of liposomes produced by ultrasonication and coated with pectin for the coencapsulation of vitamins D3 and B12, Food Chem 485 (2025) 144441, https://doi.org/10.1016/J.FOODCHEM.2025.144441.

[15] I.N. Gostin, I.E. Popescu, Evaluation of the essential oils used in the production of biopesticides: assessing their toxicity toward both arthropod target species and beneficial pollinators, Agriculture 14 (2023) 81, https://doi.org/10.3390/AGRICULTURE14010081.

[16] P. Gupta, S. Preet, Ananya, N. Singh, Preparation of Thymus vulgaris (L.) essential oil nanoemulsion and its chitosan encapsulation for controlling mosquito vectors, Sci. Rep 12 (2022) 1–14, https://doi.org/10.1038/S41598-022-07676-5;SUBJMETA=601,631,692,699;KWRD=DISEASES,ZOOLOGY.

[17] C.T. Hill, R.F. Tabor, Properties of scalable, pH-sensitive chitosan polymer-stabilised emulsions, J. Mol. Liq. 433 (2025) 127888, https://doi.org/10.1016/J.MOLLIQ.2025.127888.
[18] Y.-R. Lai, C.-H. Lin, C.-P. Chang, H.-F. Ni, W.-S. Tsai, C.-J. Huang, Y-R, L, C-h, L, C-p, C, H-f, N, W-s, T, C-j, H, Distribution of copper resistance gene variants of Xanthomonas citri subsp. citri and Xanthomonas euvesicatoria pv. perforans, Plant Prot. Sci. 57 (2021) 206–216, https://doi.org/10.17221/160/2020-PPS.
[19] T. Liu, L. Liu, Fabrication and characterization of chitosan nanoemulsions loading thymol or thyme essential oil for the preservation of refrigerated pork, Int. J. Biol. Macromol 162 (2020) 1509–1515, https://doi.org/10.1016/J.IJBIOMAC.2020.07.207.
[20] R.L. Luneja, A.G. Mkindi, Advances in botanical-based nanoformulations for sustainable cotton insect pest management in developing countries, Front. Agron. 7 (2025) 1558395, https://doi.org/10.3389/FAGRO.2025.1558395/BIBTEX.
[21] D.T. Machado, D.A. Moraes, N.M. Santos, F.B. Ometto, E.A. Ticianelli, L. C. Varanda, Wet-chemistry synthesis of ultrasmall α-MoC1-x nanoparticles and rGO/α-MoC1-x composite and its evaluation as electrocatalysts for hydrogen evolution reaction, Mater. Res. Bull 174 (2024) 112737, https://doi.org/10.1016/J.MATERRESBULL.2024.112737.
[22] F.J. Machado, T.G. Marin, S. da, F. CanÔas, G.J. da Silva Junior, F. Behlau, Timing of copper sprays to protect mechanical wounds against infection by Xanthomonas citri subsp. citri, causal agent of citrus canker, Eur. J. Plant Pathol 160 (2021) 683–692, https://doi.org/10.1007/S10658-021-02276-X/FIGURES/4.
[23] T.G.S. Marin, A.L. Galvanin, F.E. Lanza, F. Behlau, Description of copper tolerant Xanthomonas citri subsp. citri and genotypic comparison with sensitive and resistant strains, Plant Pathol 68 (2019) 1088–1098, https://doi.org/10.1111/PPA.13026;PAGEGROUP:STRING:PUBLICATION.
[24] F. Mendiburu Statistical Procedures for Agricultural Research. cran.r-project.org. 2023.
[25] F.-B. Meng, Z.-Z. Gou, Y.-C. Li, L.-H. Zou, W.-J. Chen, D.-Y. Liu, F.-B. Meng, Z.-Z. Gou, Y.-C. Li, L.-H. Zou, W.-J. Chen, Da-Yu Liu, The efficiency of lemon essential oil-based nanoemulsions on the inhibition of Phomopsis sp. and reduction of postharvest decay of kiwifruit, Foods 11 (2022) 1510, https://doi.org/10.3390/FOODS11101510.
[26] A. Modafferi, G. Giunti, G. Benelli, O. Campolo, Ecological costs of botanical nano-insecticides, Curr. Opin. Environ. Sci. Health 42 (2024) 100579, https://doi.org/10.1016/J.COESH.2024.100579.
[27] M. MondÉjar-LÓpez, A.J. LÓpez-Jimenez, J.C. GarcÍa MartÍnez, O. Ahrazem, L. GÓmez-GÓmez, E. Niza, Comparative evaluation of carvacrol and eugenol chitosan nanoparticles as eco-friendly preservative agents in cosmetics, Int. J. Biol. Macromol 206 (2022) 288–297, https://doi.org/10.1016/J.IJBIOMAC.2022.02.164.
[28] R.A. Moral, J. Hinde, C.G.B. DemÉtrio, Half-normal plots and overdispersed models in R: The hnp Package, J. Stat. Softw 81 (2017) 1–23, https://doi.org/10.18637/JSS.V081.I10.
[29] L.G. MorÃo, C.R. Polaquini, M. Kopacz, G.S. Torrezan, G.M. Ayusso, G. Dilarri, L. B. Cavalca, A. Zielińska, D.J. Scheffers, L.O. Regasini, H. Ferreira, A simplified curcumin targets the membrane of Bacillus subtilis, Microbiologyopen 8 (2019), https://doi.org/10.1002/MBO3.683.
[30] A. Mushtaq, S. Mohd Wani, A.R. Malik, A. Gull, S. Ramniwas, G. Ahmad Nayik, S. Ercisli, R. Alina Marc, R. Ullah, A. Bari, Recent insights into nanoemulsions: their preparation, properties and applications, Food Chem. X 18 (2023) 100684, https://doi.org/10.1016/J.FOCHX.2023.100684.
[31] M. Rayan, S. Abu Lafi, M. Falah, T. Kacergius, A. Kirkliauskiene, V. Gabe, A. Rayan, Alkyl Gallates as potential antibiofilm agents: a review, Molecules 28 (2023) 1751, https://doi.org/10.3390/MOLECULES28041751.
[32] R. RomÁn-Doval, S.P. Torres-Arellanes, A.Y. Tenorio-Barajas, A. GÓmez-SÁnchez, A.A. Valencia-Lazcano, Chitosan: properties and its application in agriculture in context of molecular weight, Polymers 15 (2023) 2867, https://doi.org/10.3390/POLYM15132867.
[33] F. Salehi, H. Behboudi, G. Kavoosi, S.K. Ardestani, Incorporation of Zataria multiflora essential oil into chitosan biopolymer nanoparticles: a nanoemulsion based delivery system to improve the in-vitro efficacy, stability and anticancer activity of ZEO against breast cancer cells, Int. J. Biol. Macromol. 143 (2020) 382–392, https://doi.org/10.1016/J.IJBIOMAC.2019.12.058.
[34] A. Savietto, C.R. Polaquini, M. Kopacz, D.J. Scheffers, B.C. Marques, L.O. Regasini, H. Ferreira, Antibacterial activity of monoacetylated alkyl gallates against Xanthomonas citri subsp. citri, 2018 200:6, Arch. Microbiol. 200 (2018) 929–937, https://doi.org/10.1007/s00203-018-1502-6.
[35] J. Schindelin, I. Arganda-Carreras, E. Frise, V. Kaynig, M. Longair, T. Pietzsch, S. Preibisch, C. Rueden, S. Saalfeld, B. Schmid, J.Y. Tinevez, D.J. White, V. Hartenstein, K. Eliceiri, P. Tomancak, A. Cardona, Fiji: an open-source platform for biological-image analysis, Nat. Methods 9 (2012) 676–682, https://doi.org/10.1038/nmeth.2019.
[36] Y. Shao, C. Wu, T. Wu, Y. Li, S. Chen, C. Yuan, Y. Hu, Eugenol-chitosan nanoemulsions by ultrasound-mediated emulsification: formulation, characterization and antimicrobial activity, Carbohydr. Polym. 193 (2018) 144–152, https://doi.org/10.1016/J.CARBPOL.2018.03.101.
[37] Y. gang Shi, R. run Zhang, C. min Zhu, X. rui Liang, R. Ettelaie, L. Jiang, S. Lin, On the mechanism behind enhanced antibacterial activity of alkyl gallate esters against foodborne pathogens and its application in Chinese icefish preservation, Food Microbiol. 99 (2021) 103817, https://doi.org/10.1016/J.FM.2021.103817.
[38] I.C. Silva, L.O. Regasini, M.S. PetrÃnio, D.H.S. Silva, V.S. Bolzani, J. Belasque, L.V. S. Sacramento, H. Ferreira, Antibacterial activity of alkyl gallates against Xanthomonas citri subsp. citri, J. Bacteriol. 195 (2013) 85, https://doi.org/10.1128/JB.01442-12.
[39] J. Stetefeld, S.A. McKenna, T.R. Patel, Dynamic light scattering: a practical guide and applications in biomedical sciences, Biophys. Rev. 8 (2016) 409–427, https://doi.org/10.1007/S12551-016-0218-6/FIGURES/6.
[40] The R Core Team, 2025. R: A Language and Environment for Statistical Computing. cran.r-project.org.
[41] N. Thungphotrakul, P. Prapainainar, Development of polyvinyl alcohol/carboxymethylcellulose-based bio-packaging film with citric acid crosslinking and clove essential oil encapsulated chitosan nanoparticle pickering emulsion, Int. J. Biol. Macromol 282 (2024) 137223, https://doi.org/10.1016/J.IJBIOMAC.2024.137223.
[42] S. Woranuch, R. Yoksan, Eugenol-loaded chitosan nanoparticles: I. Thermal stability improvement of eugenol through encapsulation, Carbohydr. Polym. 96 (2013) 578–585, https://doi.org/10.1016/J.CARBPOL.2012.08.117.
[43] K. Zaharioudakis, C.E. Salmas, N.D. Andritsos, E. Kollia, A. Leontiou, V. K. Karabagias, A. Karydis-Messinis, D. Moschovas, N.E. Zafeiropoulos, A. Avgeropoulos, C. Proestos, A.E. Giannakas, Carvacrol, citral, eugenol and cinnamaldehyde casein based edible nanoemulsions as novel sustainable active coatings for fresh pork tenderloin meat preservation, Front. Food Sci. Technol. 4 (2024) 1400224, https://doi.org/10.3389/FRFST.2024.1400224/BIBTEX.
[44] C.F.C. Zamuner, V.R. Marin, G. Dilarri, G.B. Hypolito, D.C. Sass, H. Ferreira, Oregano essential oil and its main components Thymol and Carvacrol as alternatives to control citrus canker, Front. Agron. 5 (2023) 1148969, https://doi.org/10.3389/FAGRO.2023.1148969.